Functional stability of coastal plankton communities toward extreme weatherrelated stressors

Soulié Tanguy*¹, Vidussi Francesca¹, Mostajir Behzad*¹

 1 MARBEC (MARine Biodiversity, Exploitation, and Conservation), Univ Montpellier, CNRS, Ifremer, IRD – Montpellier, France

*Corresponding authors

Correspondence: tanguy.soulie@gmail.com, Behzad.mostajir@umontpellier.fr

Short title: Plankton responses toward heatwave and runoff

17 Abstract

Extreme weather events, such as marine heatwaves and terrestrial runoff, are intensifying in many areas and pose growing threats. In the present study, we assessed the functional stability of plankton communities in response to these events by comparing their responses to marine heatwave and terrestrial runoff stressors. Using two in situ mesocosm experiments conducted at the same coastal site, we examined two key functional balances, namely, the metabolic balance between gross primary production (GPP) and community respiration (R), and the trophic balance between phytoplankton growth (μ) and losses (L). Plankton showed higher resistance to the heatwave than to the runoff, with smaller changes in GPP, R, μ , and L. However, functional resilience was limited after the heatwave, while the community rapidly recovered from the runoff, with overcompensation of all investigated parameters. Respiration responses were similar under both disturbances despite contrasting environmental changes in light, temperature, and nutrients. Our results highlight complex patterns of short-term functional stability in response to extreme events and underscore the need to consider both resistance and resilience when evaluating ecosystem responses to climate change. These insights could inform future monitoring and management strategies for vulnerable coastal waters.

Keywords: Plankton, Functional stability, Resistance, Resilience, Climate Change, Mesocosm, Metabolism

33 Introduction

In recent decades, the frequency and intensity of extreme weather events have increased substantially,
largely driven by global climate change (Ummenhofer & Meehl, 2017). Among the marine ecosystems,
coastal systems are particularly exposed to extreme weather events because of their proximity to both
terrestrial and marine forcings. This makes them especially vulnerable to cumulative impacts (Halpern et
al., 2019). The Mediterranean Sea, a biodiversity hotspot and a critical component of the global marine
ecosystem, faces growing threats from extreme weather events (Lejeusne et al., 2010; Darmaraki et al.,
2024). Marine heatwaves, which are characterized by prolonged periods of abnormally high sea
temperatures, have been linked to mass mortality events among marine species, disruption of reproductive
cycles, and shifts in species distribution (Garrabou et al., 2022; Darmaraki et al., 2024). Intense storms
and heavy rainfall can lead to increased runoff of terrestrial matter into coastal waters. These events have
important consequences for marine ecosystems, as they alter the physical and chemical properties of the
water column, which can have cascading effects throughout the food web (Liess et al., 2016; Courboulès
et al., 2023). Although plankton communities can respond rapidly to environmental changes (Hays et al.,
2005; Beaugrand et al., 2009), extreme events may exceed their adaptive capacities (Sauterey et al., 2023;
Helbling et al., 2024), putting at risk their essential roles in ecosystems and biogeochemical cycles.
Among these key roles, phytoplankton generate oxygen through photosynthesis, a process known as
gross primary production (GPP) (Falkowski et al., 2003; Basu et al., 2018). Simultaneously, all plankton
consume oxygen through aerobic respiration (R) (Robinson et al., 2002; Robinson & Williams 2005).
Hence, the ratio between GPP and R serves as a metabolic index for aquatic systems, indicating their capacity
to function as either net consumers (GPP < R) or net producers of oxygen (GPP > R) (Serret et al., 2015).
In turn, this index is partly regulated by the growth (μ) and loss (L) rates of phyto-plankton, whose ratio
provides a trophic index of the system, reflecting the fitness of phytoplankton and its factors of loss, such as
predation, viral lysis, and other sources of loss (natural mortality, sedimentation) (Brussaard 2004; Calbet
& Landry 2004). In this regard, both metabolic and trophic indices are key parameters for characterizing
and managing the health and functioning of coastal environments (Duarte et al., 2002; Jankowski et al.,
2021; Mantikci et al., 2024), and notably Mediterranean coastal lagoons (Bas-Silvestre et al., 2024).
Despite the increasing recognition of the impacts of marine heatwaves and terrestrial runoffs on coastal

ecosystems, there remains a gap in comprehensive studies that compare the effects of MHWs and/or

terrestrial runoff on key processes mediated by plankton communities. Increases in marine heatwave intensity and frequency were linked to a decrease in phytoplankton production in nutrient-depleted areas (Cabrerizo et al., 2022), while experimental heatwaves resulted in significant changes in plankton communities' structure (Filiz et al., 2020; Ahme et al., 2024; Huỳnh et al., 2024) and metabolism (Jeppesen et al., 2020; Soulié et al., 2022a; 2023a) in various aquatic systems. Similarly, terrestrial runoffs were shown to change plankton community structure in coastal waters (Meunier et al., 2017; Mustaffa et al., 2020; Courboulès et al., 2023; Meyneng et al., 2024) and affect plankton metabolic and trophic parameters (Rodríguez et al., 2016; Trinh et al., 2016; Soulié et al., 2024; Rowe et al., 2025).

Functional stability metrics, namely resistance, that is, the ability of a given ecosystem function to withstand a disturbance (Hillebrand et al., 2018); resilience, that is, the speed and direction of recovery of that function from change (Hillebrand et al., 2018); and final recovery success, that is, the legacy of the disturbance on the given function; are key parameters for quantifying the ability of an ecosystem to absorb and recover from a disturbance. They have been increasingly used in the framework of plankton communities' response to climate change-related disturbances, and notably during mesocosm experiments (Filiz et al., 2020; Soulié et al., 2022a; Yalçın et al., 2024). However, their use for comparing the responses to multiple disturbances remains scarce (Polazzo & Rico, 2021).

Addressing environmental challenges has become more critical than ever to safeguard water quality and preserve marine ecosystems, particularly vulnerable coastal waters, and the services they provide. In this study, we used the metabolic and trophic indices of the plankton community of a coastal Mediterranean lagoon (Thau Lagoon) to compare how heatwaves and terrestrial runoff affect the health and functioning of coastal ecosystems. We used high-frequency data acquired by automated sensors during two in situ mesocosm experiments performed in spring of 2019 and 2021 at the same site and with the same experimental setup to calculate both metabolic and trophic indices, as well as their resistance, resilience, and final recovery toward both heatwaves and terrestrial runoffs. Dissolved nutrient concentrations, bacterial abundance, and phytoplankton pigment concentrations were assessed by daily manual sampling of the mesocosms.

In situ mesocosm experiments

Two *in situ* mesocosm experiments were performed in the Mediterranean coastal lagoon of Thau (South of France). Both experiments were carried out at the same facilities of the Mediterranean platform for Marine Ecosystem Experimental Research (43°24'53"N; 3°41'16"E). The first experiment was performed to simulate a marine heatwave from May 24th to June 12th, 2019 (Soulié *et al.*, 2022a). Hereafter, this experiment will be referred to as the heatwave (HW) experiment. A second experiment was performed to simulate a terrestrial runoff event from May 3rd to May 21st, 2021 (Courboulès *et al.*, 2023; Soulié *et al.*, 2024). Hereafter, this experiment will be referred to as the terrestrial runoff (T. runoff) experiment. For each experiment, mesocosms consisted of transparent bags made of 200-µm thick vinyl acetate polyethylene film reinforced with nylon (Insinööritoimisto Haikonen Ky, Sipoo, Finland). To avoid external inputs, the mesocosms were covered with a polyvinyl-chloride dome, transmitting 73% of the photosynthetically available radiation (PAR).

On the first day of each experiment, the mesocosms were filled with 2200 L of subsurface lagoon water using a pump (SXM2/ASG; Flygt). The sampled water was previously screened on a 1000 µm mesh to remove large particles and organisms. The homogeneity of the different mesocosms during the filling procedure was ensured by simultaneously distributing the sampled water by gravity into all the mesocosms through parallel pipes. For each experiment, the water column of the mesocosms was maintained homogenous by gentle mixing with a pump (Model 360, Rule) immersed at a depth of 1 m, which resulted in a turnover rate of approximately 3.5 d⁻¹. A detailed description of the mesocosms and filling procedure can be found in **Soulié** *et al.* (2022a) for the HW experiment and in **Courboulès** *et al.* (2023) for the T. Runoff experiment.

Experimental treatments

During the HW experiment, three mesocosms served as controls, and their water temperature followed the natural water temperature of the lagoon. In three other mesocosms, a marine heatwave was simulated by heating their water column temperature at +3°C compared to the control mesocosms for the first 10 days of the experiment (d1-d10). For the last nine days of the experiment (d11-d19), their water temperature was returned to that of the control mesocosms. Heating was performed using a submersible heating element

(Galvatec) placed at a depth of 1 m. Details regarding the experimental treatment and procedures can be found in **Soulié** *et al.* (2022a).

During the T. Runoff experiment, maturated soil was added in duplicate mesocosms to simulate a terrestrial runoff event, whereas two other mesocosms served as controls and did not receive any addition. Soil from the Puéchabon oak forest (43°44'29"N; 3°35'45"E) was maturated in water from the Vène river, the main tributary of Thau Lagoon, for 14 days, before being added to the T. Runoff mesocosms on d1. Soil extraction, preparation, and maturation procedures were performed to closely mimic natural terrestrial runoff events occurring in Thau Lagoon. The details of the experimental treatment and procedures can be found in Courboulès *et al.* (2023) and Soulié *et al.* (2024).

Acquisition, calibration, and correction of high-frequency sensor measurements

For both mesocosm experiments, a set of high-frequency sensor measurements was immersed in each mesocosm at a depth of 1 m. This set consisted of sensors measuring the dissolved oxygen concentration and saturation (Aanderaa 3835), chlorophyll-*a* (Chl-*a*) fluorescence (WetLabs ECO-FLNTU), conductivity (Aanderaa 4319), PAR (Li-Cor Li-193), and water temperature (Campbell Scientific Thermistore Probe 107). The measurements of all sensors were performed at a frequency of one measurement per minute for the entire duration of the experiments. Sensors measuring the dissolved oxygen concentrations, Chl-*a* fluorescence, salinity, and temperature were calibrated before and after the experiments. The sensor calibration procedures for the HW and T. Runoff experiments can be found elsewhere (Soulié *et al.*, 2022a; 2024). Following the procedure described by Bittig *et al.* (2018), dissolved oxygen concentration data were corrected using salinity and temperature measurements. Following Soulié *et al.* (2021), dissolved oxygen concentration data were also corrected with discrete dissolved oxygen concentration measurements performed using Winkler's method. Chl-*a* fluorescence data were corrected with discrete Chl-*a* concentration measurements performed using high performance liquid chromatography (HPLC). In addition, the Chl-*a* fluorescence data were corrected for non-photochemical quenching by linearly interpolating the data from sunrise to sunset (Mitchell *et al.*, 2024).

Dissolved nutrients, phytoplankton pigment concentrations, and bacterial abundances from manual sampling of the mesocosms

All mesocosms were sampled daily using a 5 L Niskin water sampler between 09:00 and 10:00 in the morning for dissolved nutrient and phytoplankton pigment concentrations during both experiments. For dissolved inorganic nutrients (nitrite + nitrate NO₂⁻ + NO₃⁻, ammonium NH₄⁺, orthophosphate PO₄³-, silicate SiO₂), subsamples of 50 mL were put into acid-washed polycarbonate bottles, then filtered through 0.45 μm filters (Gelman) and stored at -20°C until analyses. Nitrite, nitrate, orthophosphate, and silicate concentrations were measured using an automated colorimeter (Skalar Analytical) (**Aminot & Kérouel, 2007**), and ammonium concentrations were determined using the fluorometric method (Turner Design) (**Holmes** *et al.*, **1999**).

For phytoplankton pigment analyses, subsamples of 800-1200 mL were put into covered acid-washed 2 L bottles, then filtered through 0.7 μm filters (Whatman GF/F) at a low vacuum setting and stored at -80°C until analyses. Pigment concentrations were measured with HPLC (HW experiment: Waters, T. Runoff experiment: Shimadzu) following the method of **Zapata** *et al.* (2000). Attribution of specific pigment biomarkers to phytoplankton functional types was done following **Vidussi** *et al.* (2000) and **Roy** *et al.* (2011). More precisely, fucoxanthin was attributed to diatoms, 19'-hexanoyloxyfucoxanthin (19'-HF) to prymnesiophytes, zeaxanthin to cyanobacteria, and chlorophyll-*b* (Chl-*b*) to green algae.

Subsamples (1.5 mL) were also taken to count heterotrophic bacteria by flow cytometry. The samples were fixed with glutaraldehyde (Grade 1, 4% final concentration), before being frozen at -80°C until analysis. Bacteria were stained with SYBR Green I (0.25%, final concentration), before analysis using a FACSCanto flow cytometer. Counting and identification were performed using induced fluorescence (530/30 nm). See **Courboulès** *et al.* (2023) for further details.

Estimations of community oxygen metabolism and phytoplankton growth and loss rates from high-frequency sensor measurements

Calibrated and corrected dissolved oxygen sensor measurements were used to estimate Gross Primary Production (GPP) and community Respiration (R) using the method described by **Soulié** *et al.* (2021), which is based on the free-water diel oxygen technique (**Staehr** *et al.*, 2010). Calibrated and corrected Chl-*a* fluorescence sensor measurements were used to estimate phytoplankton growth rate (μ) and phytoplankton

loss rate (L) using the method of Soulié et al. (2022b). Detailed descriptions of both methods are provided in Soulié et al. (2022a, 2024).

176 177

179

174

175

Estimations of daily light integral from high-frequency sensor measurements

178 The Daily Light Integral (DLI) was calculated from high-frequency PAR measurements using the following equation (Eq. 1):

$$DLI = \frac{PAR \times day \ length \times 3600}{1 \times 10^6} \ (Eq. 1)$$

DLI is expressed in mol m⁻² d⁻¹, PAR, representing the average PAR value from sunrise to sunset, in µmol 181 m⁻² s⁻¹, and day length in h (Soulié et al., 2022a). 182

183 184

Data analyses

185 186 187

188

189

All the data treatments and analyses were performed using R software (version 4.1.0). For comparing the experiments, all the data were normalized by the control values for both experiments. To do so, the Logarithmic Response Ratio (LRR) was calculated with the following equation (Eq. 2):

$$LRR_X = \log\left(\frac{X_{TREAT}}{X_{CONT}}\right) (Eq. 2)$$

191

192

193

194

195

196

197

198

199

200

201

where, LRR_X represents the LRR of the X variable, X_{TREAT} represents the average value of X for the treated mesocosms (heated mesocosms for the HW experiment, and mesocosms in which the terrestrial runoff was simulated for the T. Runoff experiment), and X_{CONT} represents the average value of X for the control mesocosms. Note that the values are the average of three replicates for the HW experiment and two replicates for the T. Runoff experiment. A value of 0 for LRR_X represents no difference from the control, whereas positive or negative values represent positive or negative effects of the treatments, respectively. Cohen's d effect size was used for a power analysis to compare the size of the effects of the treatments between the experiments. It was calculated as the difference between the average values in the treated and non-treated (control) mesocosms divided by the pooled standard deviation (Cohen 1977), using the cohensD function from the *lsr* R package (Navarro 2015). Different ranges of Cohen's d effect sizes were defined: very small between |0| and |0.2|; small between |0.2| and |0.5|; medium between |0.5| and |0.8|; large between |0.8| and |1.2|; very large higher than |1.2|.

To statistically test the differences in the LRRs between the two experiments, repeated-measures Analyses of variances (RM-ANOVA) were performed using the *nlme* R package (**Pinheiro** *et al.* **2025**). In the models, time was used as a random factor and experiment as a fixed factor. Autocorrelation was considered by adding an autoregressive process of order 1 into the model. The homoscedasticity and normality assumptions for parametric tests were checked prior by using the Levene and Shapiro–Wilk tests, respectively. When the assumptions were not met, a non-parametric Kruskal–Wallis test was performed instead of the RM- ANOVA, using the *kruskal.test* function from the *stats* package. In addition, principal component analyses (PCA) and ordinary least squares linear relationships between the LRR of GPP, R, μ, L, and Chl-*a* were performed to assess potential relationships and drivers among variables.

Stability metrics (resistance, resilience, and recovery) were calculated for both experiments following the equations of **Hillebrand** *et al.* (2018). Their mathematical definition and interpretation are presented in **Table 1** for both experiments. All the metrics were based on the LRR for different experimental periods. Note that the resistance was calculated as the immediate resistance (d2) for both the HW and T. Runoff experiments, whereas the average resistance (from d2 to d10) was calculated only for the HW experiment. For both experiments, immediate resistance was calculated on d2 as treatments (heating or addition of soil) were not applied for the entirety of d1 (starting of heating and addition of soil were performed around 11:00 on the morning of d1).

Table 1 - Stability metrics periods of calculation, mathematical definitions, and interpretations for both experiments, according to **Hillebrand** *et al.* (2018). X_{TREAT} and X_{CONT} represent the average value of X for the treatment and control mesocosm replicates, respectively.

Parameter	Period for	Period for the	Mathematical definition	Interpretation
	the HW	T. Runoff		
	experiment	experiment		
Immediate	d2	d2	$x = \ln(X_{TREAT})$	$a=0 \rightarrow$ maximum resistance
resistance (a)			$a = \ln(\frac{X_{TREAT}}{X_{CONT}})$	$a>0 \rightarrow$ overperformance
			2011	$a<0 \rightarrow$ underperformance
Average	d2-d10		$x = \ln(X_{TREAT})$	$a=0 \rightarrow$ maximum resistance
resistance (a)			$a = \ln(\frac{X_{TREAT}}{X_{CONT}})$	$a>0 \rightarrow$ overperformance
			CONT	$a<0 \rightarrow$ underperformance
Resilience	d11-d19	d3-d17	$\ln\left(\frac{X_{TREAT}}{X_{TREAT}}\right) = b \times t + i$	$b=0 \rightarrow \text{no recovery}$
(<i>b</i>)			$\lim \left(\frac{1}{X_{CONT}} \right) = b \times t + t$	$b>0 \rightarrow$ faster recovery (if $i<0$)
			CONT	$b<0 \rightarrow$ further deviation from
				the control (if $i < 0$)

Recovery (c)	d19	d17	X_{TREAT}	$a=0 \rightarrow$ maximum recovery
			$c = \ln({X_{CONT}})$	$a>0 \rightarrow$ overcompensation
			CON1	$a<0 \rightarrow incomplete recovery$

Effects of HW and T. Runoff on the metabolic and trophic indexes of plankton communities

227 Results

228229230

231

232

233

234

235

236

237

238

239

240

241

242

243

244

245

246

247

248

249

250

251

252

253

226

During the HW experiment, the logarithmic response ratio (LRR) of GPP varied from 0.01 (d1) to 0.17 (d10) during the heatwave period, peaking on d3 (0.22), corresponding to a medium effect size (Fig. 1A, Table 3). It was positive throughout the entire period. Similarly, it was positive seven days out of nine during the recovery period (d11-d19), ranging from 0.03 on d11 to -0.04 on d19, corresponding to a large effect size. During the T. Runoff experiment, the LRR of GPP varied from -0.03 on d1, when the terrestrial runoff was simulated, to 0.01 on d17 (Fig. 1A). It was positive 13 days out of 17, displaying a sharp decrease on d2 (-0.25) and then increasing to a maximum of 0.18 on d11. Overall, the effect of the T. Runoff on GPP was of small magnitude (Table 3). The LRRs of GPP were significantly different during the HW and T. Runoff experiments, regardless of the period considered (Table 2). The LRR of R varied from -0.02 on d1 to 0.13 on d10 during the heatwave period of the HW experiment, peaking on d7 at 0.26 (Fig. 1B). It was positive during the entire period except on d1; and was calculated as a very large effect size (Table 3). During the recovery period, it varied from 0.05 on d11 to 0.05 on d19, with negative values on d13 (+0.03) and d18 (-0.09). During the T. Runoff experiment, the LRR of R varied from -0.02 on d1 to 0.08 on d17 (Fig. 1B). It was positive during the entire experiment, except on d1. The LRRs of R were not significantly different between the HW and the T. Runoff experiments, regardless of the period considered (Table 2). The GPP:R ratio displayed a small sized effect during the HW experiment, with a LRR varying from 0.02 on d1 to 0.05 on d10 for the HW period, and varying from -0.02 (d11) to -0.09 (d19) during the resilience period (Fig. 1C, Table 3). During the T. Runoff experiment, it decreased from d1 (-0.01) until d3 (-0.29), before increasing toward positive values on d11 (0.01). Overall, it displayed a medium-sized response (Table 3). The responses of GPP:R ratio were significantly different depending on the experiment (Table 2). During the HW experiment, Chl-a displayed a very small response, its LRR varied from -0.04 (d1) to -0.11 (d19) (Fig. 1D). In contrast, the effect of the T. Runoff treatment on Chl-a was of medium size and significantly different from the response during the HW experiment (Table 2, 3), with a LRR ranging from -0.1 (d1) to -0.08 (d18). Similarly, the effect of the HW on bacterial abundance was very small (Fig. 1E), while its

response during the T. Runoff experiment was larger, but no significant difference was found between experiments.

When normalized to Chl-*a*, both GPP:Chl-*a* (**Fig. 1F**) and R:Chl-*a* (**Fig. 1H**) showed similar trends in both experiments. During the HW experiment, their LRRs ranged from 0.04 and 0.02 (d1) to 0.15 and 0.2 (d19), respectively, corresponding to medium effect sizes (**Table 3**). In contrast, during the T. Runoff experiment, the LRRs of GPP:Chl-*a* and R:Chl-*a* indicated a large positive response from d3 (0.26 and 0.55, respectively) to d13 (0.21 and 0.19, respectively). Both processes showed a significantly different response between experiments (**Table 2**). When normalized by bacterial abundance, GPP:Bacteria (**Fig. 1G**) and R:Bacteria (**Fig. 1I**) showed a significantly different pattern of response between experiments from d1 to d10, with a stronger effect reported overall during the HW than the T. Runoff experiment for both variables (**Table 2, 3**).

During the HW experiment, the LRRs of μ , L, and μ :L, all displayed a relatively constant response and very small or small effects (**Table 3**), ranging from 0.03, 0.01, and 0.03 on d1, respectively, to -0.18, -0.13, and -0.06 on d19, respectively (**Fig. 1J, K, L**). In contrast, during the T. Runoff experiment, the LRRs of μ and L exhibited a sharp decrease during the first half of the experiment, reaching values of -1.03 and -1.19 on d5. After, the LRR of μ increased and even displayed a strong positive response, reaching 0.90 on d15, while the LRR of L also increased but stayed close to 0. Consequently, the LRR of the μ :L ratio ranged from -0.63 (d1) to 0.53 (d18). The LRR of μ was significantly different between experiments during the first half of the experiments (d1-d10), and the LRRs of L and μ :L were significantly different when considering the entire experiments (**Table 2**).

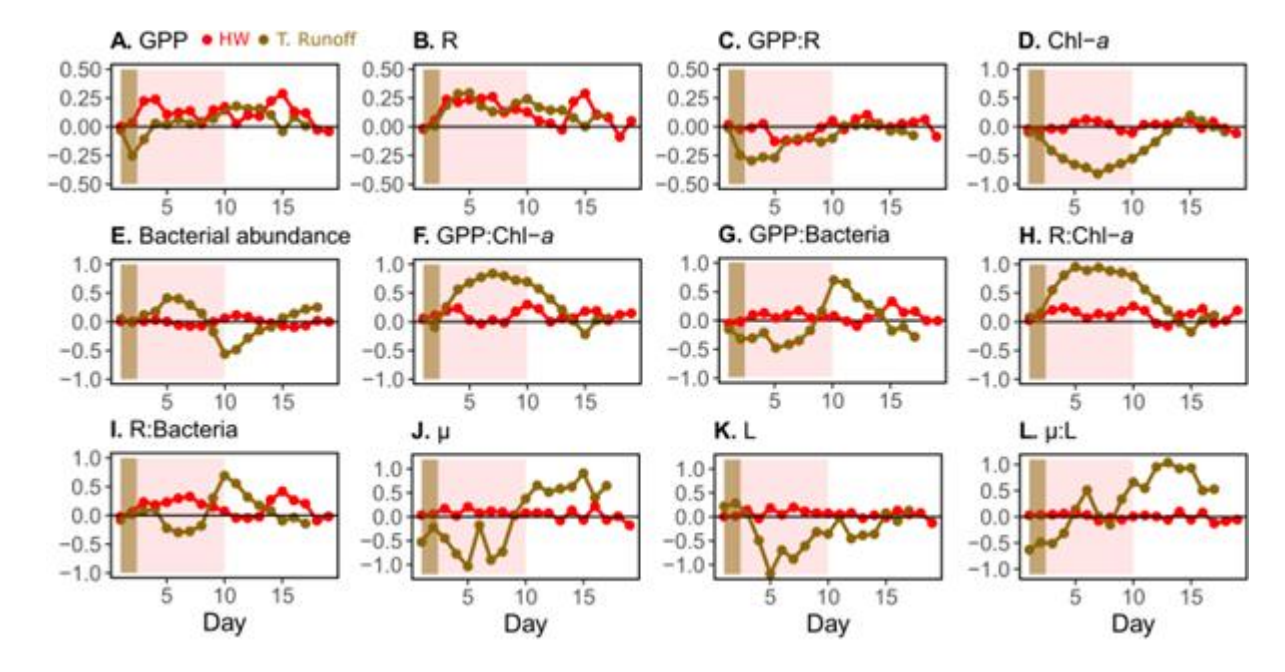


Figure 1 - Logarithm Response Ratio (LRR) of Gross Primary Production (GPP, A.), Respiration (R, B.), GPP:R (C.), chlorophyll-a (Chl-a, D.), bacterial abundance (E.), GPP normalized by Chl-a (F.), GPP normalized by bacterial abundance (G.), R normalized by Chl-a (H.), R normalized by bacterial abundance (I.), phytoplankton growth rate (μ , J.), phytoplankton loss rate (L, K.), and μ :L (L.) during the Heatwave (HW) experiment (red) and the Terrestrial Runoff (T. Runoff) experiment (gold). The red and brown backgrounds represent resistance periods (e.g., during which the experimental treatment was fully performed (d2-d10 for the HW, d2 for the T. Runoff)).

Table 2 - Summary of the results of the statistical tests assessing the differences in the Logarithm Response Ratio (LRR) of various parameters among experiments over the entire experimental periods (d1-d19) or over the period (d1-d10) during which the HW was simulated during the HW experiment. Significant P-values (< 0.05) are highlighted in bold.

Parameter	Period	Test	P-value	
GPP	d1-d19	RM-ANOVA	0.048	
	d1-d10	RM-ANOVA	0.013	
R	d1-d19	RM-ANOVA	0.791	
	d1-d10	RM-ANOVA	0.739	
GPP:R	d1-d19	Kruskal-Wallis	0.012	
	d1-d10	RM-ANOVA	0.029	
Chl-a	d1-d19	RM-ANOVA	0.001	
	d1-d10	RM-ANOVA	0.002	
Bacteria	d1-d19	RM-ANOVA	0.213	
	d1-d10	Kruskal-Wallis	0.096	
GPP:Chl-a	d1-d19	RM-ANOVA	0.018	
	d1-d10	RM-ANOVA	0.021	
GPP:Bacteria	d1-d19	Kruskal-Wallis	0.096	
	d1-d10	Kruskal-Wallis	0.023	
R:Chl-a	d1-d19	RM-ANOVA	0.003	
	d1-d10	Kruskal-Wallis	0.005	
R:Bacteria	d1-d19	RM-ANOVA	0.471	
	d1-d10	Kruskal-Wallis	0.048	
μ	d1-d19	RM-ANOVA	0.979	
•	d1-d10	RM-ANOVA	0.017	
L	d1-d19	Kruskal-Wallis	0.009	
	d1-d10	RM-ANOVA	0.039	
μ:L	d1-d19	Kruskal-Wallis	0.068	
	d1-d10	RM-ANOVA	0.706	

Table 3 - Cohen's d effect size calculated for the effect of the treatments on plankton processes, nutrient concentrations, light, temperature, and phytoplankton pigment concentrations for the HW and T. Runoff experiments. Very small between |0| and |0.2| (white); small between |0.2| and |0.5| (light blue); medium between |0.5| and |0.8| (medium blue); large between |0.8| and |1.2| (navy blue); very large higher than |1.2| (dark blue).

	HW (d1-d19)	HW (d1-d10)	HW (d11-d19)	T. Runoff (d1-d17)
GPP	0.72	0.78	0.81	0.35
R	0.90	1.48	0.75	0.89
GPP:R	0.21	0.66	0.36	0.73
Chl-a	0.05	0.02	0.38	0.60
Bacteria	0.04	0.02	0.10	0.39
GPP:Chl-a	0.46	0.47	0.80	1.04
GPP:Bacteria	0.59	0.71	0.68	0.36
R:Chl-a	0.46	0.82	0.66	1.17
R:Bacteria	0.64	0.58	1.19	0.33
μ	0.26	0.82	0.05	0.53
L	0.36	0.60	0.12	0.43
μ:L	0.04	0.21	0.21	0.75
NO ₂ -+NO ₃ -	0.23	0.26	0.26	0.09
$\mathrm{NH_{4}^{+}}$	0.24	0.38	0.04	1.33
PO_4^{3-}	0.12	0.46	0.33	0.76
SiO_2	0.36	0.94	0.06	6.60
DLI	0.42	0.49	0.33	2.04
Temperature	1.83	6.80	0.01	0.09
Fucoxanthin	0.16	0.28	0.01	0.22
19'-HF	0.22	0.30	0.74	0.60
Zeaxanthin	0.26	0.10	0.64	0.27
Chl-b	0.05	0.00	0.30	0.26

Effects of HW and T. Runoff on abiotic environmental variables

During the HW experiment, the LRRs of the dissolved nutrients exhibited various trends (**Fig. 2A-D**). During the HW period, the LRR of nitrate and nitrite (NO₂-+NO₃-) stayed relatively constant, ranging from 0.05 (d2) to 0.06 (d10). Meanwhile, during the resilience period, it showed a higher variability, ranging from 0.13 (d11) to 0.01 (d19) (**Fig. 2A**). The effect size was small in both periods (**Table 3**). During the T. Runoff experiment, it ranged from 0.06 (d1) to 0.01 (d18), displaying a very small effect size. Ammonium (NH₄+) LRR displayed a very different trend depending on the experiment (**Fig. 2B**). It was constant and corresponded to a small effect size, ranging from 0.13 (d2) to -0.06 (d19). Conversely, during the T. Runoff experiment, it increased strongly from d1 (0.03) to 1.22 (d12), before decreasing again until d18 (-0.08). Consequently, the effect size was very large (**Table 3**). Orthophosphate (PO₄³⁻) LRR minimum was attained on d5 (-0.62) during the HW experiment, while it also peaked on d9, reaching 0.97 (**Fig. 2C**). Besides these extremes, it remained relatively constant, corresponding to a very small effect size (**Table 3**). Similarly, it varied from 0.09 (d1) to 0.26 (d18) during the T. Runoff experiment, with stronger positive values during the second part of the T. Runoff experiment, resulting in an overall medium effect size (**Table 3**). Silicate (SiO₂) LRR displayed an overall decreasing trend during the HW period of the HW experiment, varying

from 0.32 (d2) to 0.02 (d10), corresponding to a large effect size (**Fig. 2D**, **Table 3**). During the resilience period, it remained relatively constant but displayed higher variability, ranging from -0.05 (d11) to 0.16 (d19). During the T. Runoff experiment, it remained positive for the entire experiment, ranging from 0.10 on d1 to 0.52 on d18, and corresponded to a very large effect size (**Table 3**). Daily Light Integral (DLI, **Fig. 2E**) and temperature (**Fig. 2F**) responded as expected to the experimental manipulations. The DLI LRR was strongest on d2 in the T. Runoff experiment (-0.62) and then increased steadily throughout the experiment, reaching -0.09 on d17, resulting in an overall very large effect size (**Table 3**). By contrast, the magnitude of its response was small during the entire HW experiment. Conversely, the LRR of temperature was very large during the HW period of the HW experiment, while it displayed a very small response during both the resilience period of the HW experiment and the T. Runoff experiment.

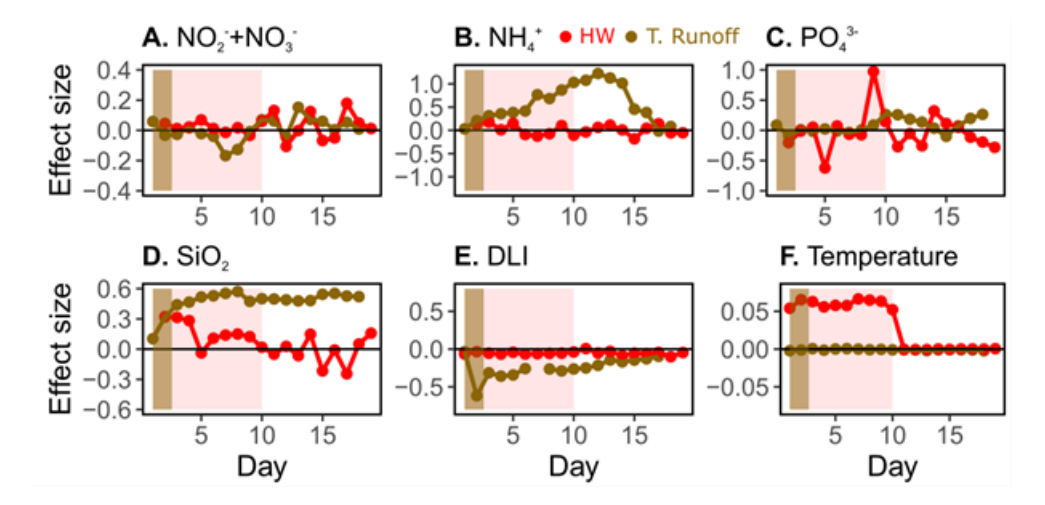


Figure 2 - Logarithm Response Ratio (LRR) of nitrite + nitrate (NO₂⁻+NO₃⁻, A.), ammonium (NH₄⁺, B.), orthophosphate (PO₄³⁻, C.), silicate (SiO₂, D.), Daily Light Integral (DLI, E.), and water temperature (F.) during the Heatwave (HW) experiment (red) and the Terrestrial Runoff (T. Runoff) experiment (gold). The red and brown backgrounds represent resistance periods (e.g., during which the experimental treatment was fully performed (d2-d10 for the HW, d2 for the T. Runoff)).

Effects of HW and T. Runoff on the phytoplankton pigment composition

During the HW experiment, the fucoxanthin and 19'-HF LRRs displayed a relatively constant trend, varying from 0.04 (d1) to 0.14 (d10) and from -0.03 (d1) to -0.04 (d10), respectively, during the HW period (**Fig. 3A, B**). However, the fucoxanthin LRR decreased strongly toward negative values by the end of the experiment, reaching -0.26 on d19. In contrast, during the T. Runoff experiment, the LRRs of fucoxanthin and 19'-HF displayed a strong negative trend, decreasing from -0.04 and -0.1 on d1, respectively, until a minimum of -1.06 on d7 for fucoxanthin and -2.3 on d5 for 19'-HF. Then, both LRRs increased again,

reaching positive values on d13 and d15, respectively. The LRR of zeaxanthin displayed similar trends as fucoxanthin and 19'-HF in both experiments, but with higher variability (**Fig. 3C**). During the HW experiment, it varied from 0.35 (d2) to -0.01 (d10) during the HW period, and from 0.28 (d11) to 0.15 (d19) during the resilience period, while, during the T. Runoff experiment, it varied from 0.22 (d1) to 0.44 (d18). The LRR of Chl-*b* varied from 0.09 (d1) to 0.01 (d10) during the HW period of the HW experiment, and displayed a strong decrease at the end of the resilience period, reaching -0.55 on d19 (**Fig. 3D**). Conversely, during the T. Runoff experiment, the Chl-*b* LRR stayed relatively constant from d1 (-0.02) to d5 (-0.09), before strongly decreasing until d8 (-0.7) before increasing again and reaching positive values from d15 (0.87). All the investigated pigment concentrations exhibited either very small, small, or medium intensity effects (**Table 3**).



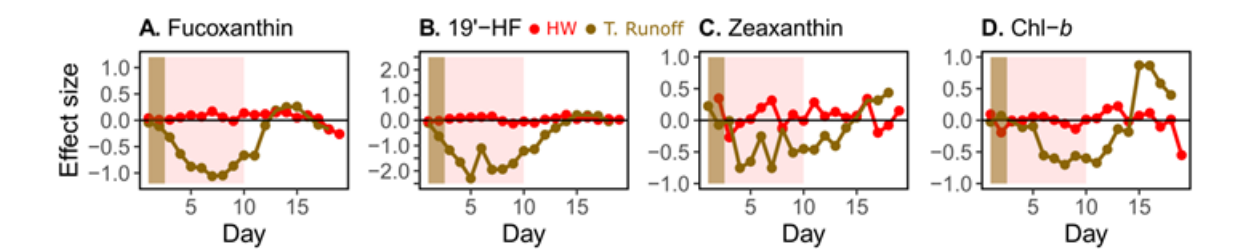


Figure 3 - Logarithm Response Ratio (LRR) of fucoxanthin (A.), 19'-hexanoloxyfucoxanthin (19'-HF, B.), zeaxanthin (C.), and chlorophyll-*b* (Chl-*b*, D.), during the Heatwave (HW) experiment (red) and the Terrestrial Runoff (T. Runoff) experiment (gold). The red and brown backgrounds represent resistance periods (e.g., during which the experimental treatment was fully performed (d2-d10 for the HW, d2 for the T. Runoff)).

Functional stability metrics during the HW and T. Runoff experiments

A summary of the functional stability metrics is presented in **Table 4**. The maximum possible resistance of a variable is zero, meaning that the values of the variable in the treatment and control mesocosms were equal when subjected to the disturbance. For the HW experiment, the best immediate resistance (calculated on d2) was found for the GPP:R ratio (-0.02) and L (0.02), while the worst was found for R:Chl-a (0.12). R displayed a worse immediate resistance (0.06) than GPP (0.03), and μ displayed a worse immediate resistance (0.05) than L (0.02). In the T. Runoff experiment, the best immediate resistance was found for R (6.9×10⁻³) and the worst for the μ :L ratio (-0.49). GPP displayed a worse resistance (-0.25) than R (0.01), and μ displayed a better resistance (-0.22) than L (0.28). Overall, the immediate resistance was worse in the T. Runoff than in the HW experiment for six parameters (GPP, GPP:R, μ , L, μ :L, R:Chl-a).

In the HW experiment, it was possible to calculate the average resistance over the entire duration of the HW (d2-d10) (**Table 1**). The best average resistance was found for μ :L (0.01) and the worst was reported for R:Bacteria (0.19). R displayed the worst average resistance (0.18) than GPP (0.13), and μ and L displayed similar average resistances (0.09).

In contrast to resistance, a resilience value of zero indicates a lack of recovery after a disturbance. In the HW experiment, all resilience values were close to zero, indicating a low resilience for all investigated parameters. The least resilient parameter was L, while the best resilience was found for μ . In the T. Runoff experiment, a strong resilience was found for μ (0.13), μ :L (0.09), and L (0.05). In contrast, a low resilience was found for GPP (0.01), R (-0.01), and GPP:R (0.02). Resilience was better for the T. Runoff than HW experiment for all investigated parameters except GPP.

Similar to the resistance, the final recovery is best when equal to zero, meaning that values in the treatment returned to the same value as observed in the control. In the HW treatment, the best recovery was reported for GPP (-0.04) and R:Bacteria (-0.02), and the worst was found for R:Chl-a (0.20). GPP displayed a better final recovery (-0.04) than R (0.05), and μ displayed a worse recovery (-0.18) than L (-0.13). In the T. Runoff experiment, the best and worst recoveries were found for GPP (7.6×10⁻³) and μ (0.65), respectively. GPP recovery was better than for R (0.08), and μ displayed a worse recovery (0.65) than L (0.13). The final recovery was found better for the HW than the T. Runoff experiment for 5 (R, GPP:Bacteria, R:Bacteria, μ , μ :L) investigated parameters out of 10.

Table 4 - Summary of the functional stability metrics (immediate resistance, average resistance, resilience, and recovery) obtained in the HW and T. Runoff experiments.

<u>Metric</u>	<u>Parameter</u>	<u>HW</u>	T. Runoff
Immediate resistance	GPP	0.03	-0.25
(The closer to 0	R	0.06	6.9×10 ⁻³
→ the better resistance)	GPP:R	-0.02	-0.25
	GPP:Chl-a	0.11	-0.09
	GPP:Bacteria	0.04	-0.24
	R:Chl-a	0.12	0.16
	R:Bacteria	0.06	0.02
	μ	0.05	-0.22
	Ĺ	0.02	0.05
	μ:L	0.04	-0.49
Average resistance	GPP	0.13	
(The closer to 0	R	0.18	
→ the better resistance)	GPP:R	-0.05	
,	GPP:Chl-a	0.11	
	GPP:Bacteria	0.13	
	R:Chl-a	0.17	
	R:Bacteria	0.19	
	μ	0.09	
	Ĺ	0.09	

	μ:L	0.01	
Resilience	GPP	-0.01	0.01
(The further from 0	R	-0.01	-0.01
→ the faster the recovery)	GPP:R	-0.01	0.01
	GPP:Chl-a	0.01	-0.03
	GPP:Bacteria	8.3×10 ⁻³	0.03
	R:Chl-a	0.01	-0.05
	R:Bacteria	6.9×10 ⁻³	8.6×10^{-3}
	μ	-0.02	0.13
	Ĺ	-9.4×10 ⁻⁴	0.05
	μ:L	-0.01	0.09
Recovery	GPP	-0.04	7.6×10 ⁻³
(The closer to 0	R	0.05	0.08
→ the closer to control values)	GPP:R	-0.09	-0.08
$(>0 \rightarrow \text{overcompensation})$	GPP:Chl-a	0.15	0.06
	GPP:Bacteria	0.06	-0.21
	R:Chl-a	0.20	0.11
	R:Bacteria	-0.02	-0.14
	μ	-0.18	0.65
	Ĺ	-0.13	0.13
	μ:L	-0.05	0.53

Relationships among biotic and abiotic variables during the HW and T. Runoff experiments

Ordinary least squares linear relationships were used to assess relationships between the effects of the treatments on the investigated parameters (**Fig. 4**). In both the HW the T. Runoff treatments, positive significant (P < 0.05) relationships were found for the effects of the treatments on GPP and R, and for μ and L (**Fig. 4A**, **B**). In contrast to the HW experiment, a significant negative relationship was found between the effects of the treatment on R and Chl-a during the T. Runoff experiment (**Fig. 4E**), and significant positive relationships were found between the effects on μ and Chl-a (**Fig. 4G**) and on L and Chl-a (**Fig. 4H**). No relationship was found between the effects of the treatment on GPP and Chl-a, GPP and bacterial abundance, and R and bacterial abundance, regardless of the experiment considered (**Fig. 4C**, **D**, **F**).

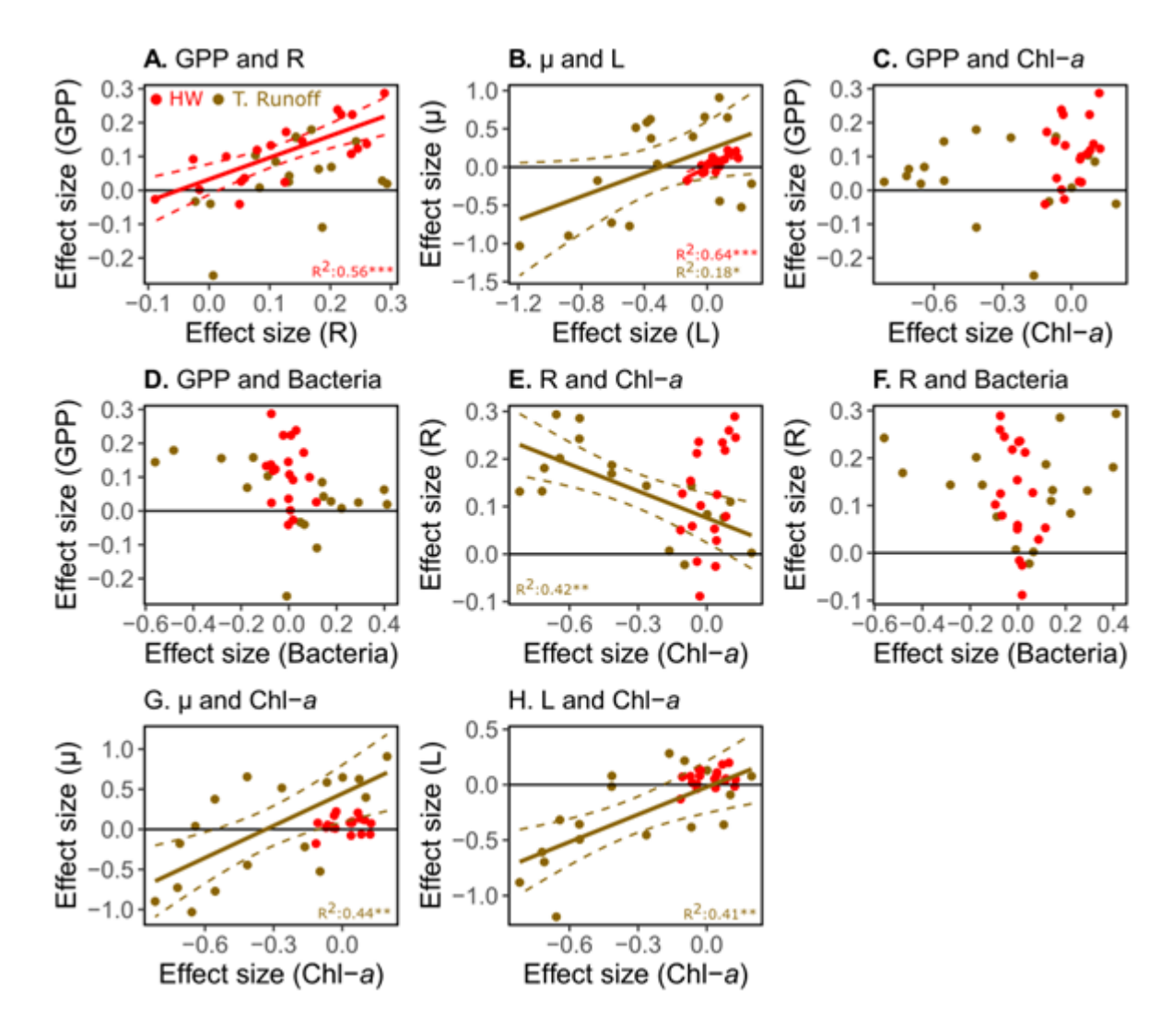


Figure 4 - Ordinary least squares linear relationships between the effect sizes of the treatment, expressed as the Logarithmic Response Ratio (LRR), on Gross Primary Production (GPP), community Respiration (R), phytoplankton growth (μ) and loss (L) rates, and chlorophyll-a concentration (Chl-a), for the HW (red) and T. Runoff (gold) experiments. Relationships were assessed individually for each experiment. Only statistically significant relationships (P < 0.05) are represented with solid and dashed lines, representing the linear least square fit and the 95% confidence interval, respectively.

PCA were performed to assess environmental and pigment drivers of the effects of the treatment on GPP, R, μ , and L, during the HW (**Fig. 5A**) and T. Runoff (**Fig. 5B**) experiments during the resilience period (d11-d19 for the HW experiment, d3-d17 for the T. Runoff experiment). The first two axes represented 52.4% and 69% of the total variance for the HW and T. Runoff experiments, respectively. For the HW experiment, the responses of GPP and R were grouped along the Dimension 1 axis with PO₄³⁻ and 19'-HF. Similarly, the responses of μ and L were clustered along the Dimension 1 axis, alongside the responses of fucoxanthin, Chl-*b*, and Chl-*a*. Both clusters appeared to be orthogonal to the response of the DLI, bacteria, SiO₂, and temperature. Finally, zeaxanthin, NO₂-+NO₃-, and NH₄+ were not well-represented by the first two

dimensions. During the T. Runoff experiment, the response of GPP during the resilience period was grouped along the Dimension 2 axis, along with the responses of NH_4^+ , and $PO_4^{3^-}$. The response of μ was clustered with the response of $NO_2^-+NO_3^-$, and the response of L was grouped along the Dimension 1 axis alongside the responses of fucoxanthin, 19'-HF, DLI, and Chl-a. Finally, the response of R was not related to any of the other variables.

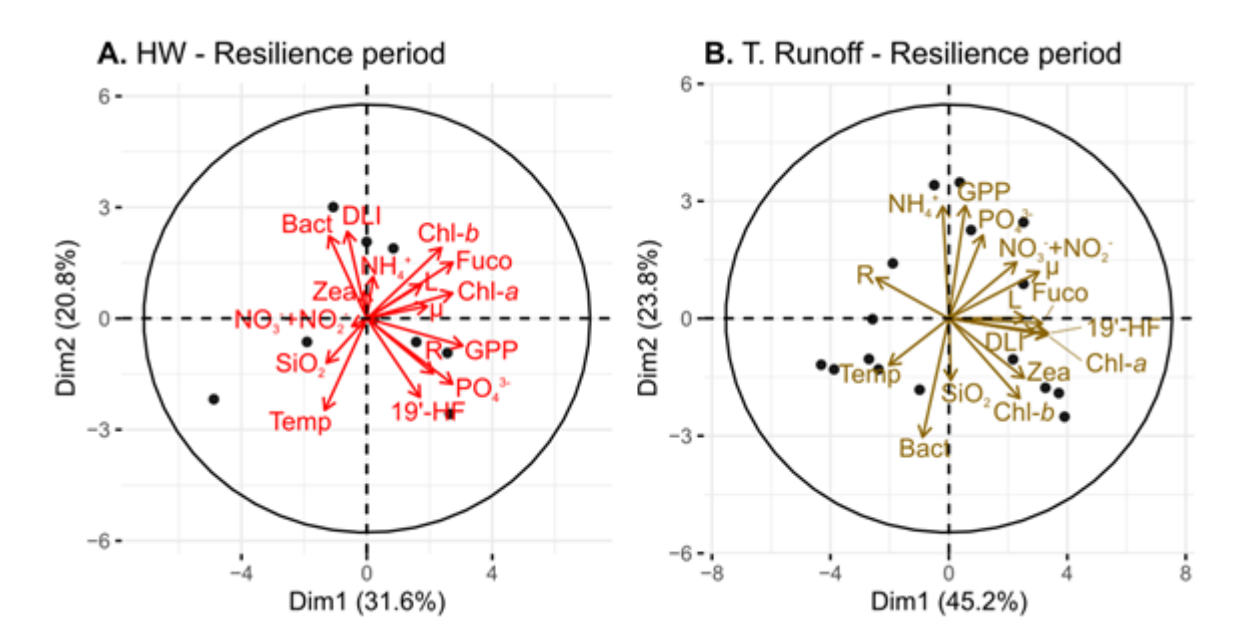


Figure 5 - Principal component analyses (PCA) between the effect sizes of the treatment, expressed as the Logarithmic Response Ratio (LRR), during the resilience period (d11-d19 for the HW experiment, d3-d17 for the T. Runoff experiment) on Gross Primary Production (GPP), community Respiration (R), phytoplankton growth (μ) and loss (L) rates, chlorophyll-a concentration (Chl-a), bacterial abundance (Bact), environmental variables (nutrient, light, and temperature) and phytoplankton pigment concentrations (Fuco: Fucoxanthin, 19'-HF: 19'-hexanoyloxyfucoxanthin, Zea: zeaxanthin, Chl-b: chlorophyll-b), for the HW (red, A.) and T. Runoff (gold, B.) experiments.

Discussion

 Plankton oxygen metabolism and phytoplankton growth and loss rates are more resistant to marine heatwaves than to terrestrial runoffs

Resistance, defined as the ability of a function to withstand a perturbation (Hillebrand et al., 2018), is a key parameter for understanding how a population, community, or ecosystem can withstand and adapt to environmental changes, highlighting the measures to be taken for conservation and management practices aimed at sustaining the good health of ecosystems. As global change continues to accelerate, the need for comprehensive resistance assessments has become increasingly urgent. To the best of our knowledge, the present study is the first to show that the resistance for all investigated plankton processes is better toward

heatwaves than toward terrestrial runoffs in a coastal Mediterranean site, regardless of considering the immediate or the average resistance for the simulated heatwave. This is certainly because of differences in the nature and intensity of the disturbances. Indeed, both disturbances are different in their nature as, in theory, terrestrial runoffs affect more phytoplankton than other organisms due to light limitation, while heatwayes affect more heterotrophs than phytoplankton due to the stronger temperature-dependence of heterotrophic metabolism (Garcia-Corral et al., 2021). Additionally, both disturbances can differ in their intensity. For example, the terrestrial runoff decreased light availability by 76% on the first day after addition (d2, when resistance was calculated) compared to control conditions, whereas the simulated heatwave increased water temperature by 15% compared to the control (Soulié et al., 2022a; 2024). However, both disturbances were designed to closely mimic natural events, and the difference in the intensity of the disturbances may be representative of what will be simulated in future scenarios. The worst resistance found for terrestrial runoffs compared to heatwaves suggests that light is a more important factor controlling the processes mediated by plankton communities, notably by phytoplankton, within coastal ecosystems such as the Thau Lagoon than temperature. This emphasizes the role of light in the regulation of phytoplankton photosynthesis and primary production, which are key ecosystem services in shallow coastal waters. This is congruent with recent meta-analyses highlighting the role of light for the functioning of plankton communities and the ecosystem services they provide (Stibor & Stockenreiter, 2023; Striebel et al., 2023). Additionally, these observations suggest that Mediterranean coastal plankton communities might be welladapted to rapid temperature variations, allowing for enhanced resistance to thermal stress, due to the shallowness and low inertia of the water column which often result in significant amplitude of daily, weekly, and monthly temperature variations (Pérez-Ruzafa et al., 2005; Ferrarin et al., 2014).

443

444

445

446

447

448

449

450

451

452

453

454

455

456

457

458

459

460

461

462

463

464

465

466

467

468

469

470

471

During the terrestrial runoff experiment, the lowest resistances were found for all processes directly related to photosynthesis, that is, primary production, Chl-*a*, and phytoplankton growth rate, suggesting a strong direct effect of the reduction in light on primary producers. These negative effects may have quickly propagated to other components of the food web, as resistance of the phytoplankton loss rate was also low. The phytoplankton loss rate encompasses both grazing from higher trophic level organisms and viral lysis, suggesting that the lack of resistance of phytoplankton and its photosynthesis toward terrestrial runoffs may rapidly impact other processes shaping coastal ecosystems. This was seen with the very low resistance for both the metabolic (GPP:R) and trophic (μ :L) indices, which displayed among the worst resistances of all

tested parameters. Both indices reflect vital processes in coastal ecosystems, related to their entire functioning and health (**Duarte** *et al.*, **2002**; **Mantikci** *et al.*, **2024**). Owing to the lack of resistance of these indices toward terrestrial runoffs, the potentially drastic consequences of such events highlight the need to develop adaptive management strategies to mitigate these consequences in coastal ecosystems, notably regarding land use and water management (**La Jeunesse** *et al.*, **2015**).

477 478

472

473

474

475

476

Contrasting resilience patterns: high resilience after the terrestrial runoff leads to functional recovery, while low resilience after the heatwave does not

479 480 481

482

483

484

485

486

487

488

489

490

491

492

493

494

495

496

497

498

499

500

501

502

During the terrestrial runoff experiment, most processes displayed a strong resilience, resulting in them returning to a level close to that observed in the control before the end of the experiment. More precisely, primary production, respiration, and their ratio (GPP:R, metabolic index of plankton community), as well as phytoplankton loss rates, returned to close-to-control conditions before the end of the experiment. This highlights the relatively short-term legacy of terrestrial runoff events in Thau Lagoon, with consequences for the aforementioned key plankton processes lasting only several days. However, the phytoplankton growth rate resilience pattern appeared to be different from that observed for the other studied processes, as resilience led to overcompensation approximately one week after the runoff. This positive response of the phytoplankton growth rate, due to concomitant decrease in light attenuation and increase in nutrient availability as shown in the PCA analysis (Soulié et al., 2024), resulted in low resilience for the trophic index of plankton community (µ:L) of the lagoon, and to poor recoveries for both the growth rate and the trophic index by the end of the experiment. These results are in agreement with observations after a natural terrestrial runoff event in Thau Lagoon, during which a mismatch between prey (i.e., phytoplankton) and predators (i.e., zooplankton) was reported due to increases in abundance of prey but not predators (Pecqueur et al., 2011). Therefore, the high resilience of community oxygen metabolism and phytoplankton loss rate observed in this study suggests that terrestrial runoffs are unlikely to have long-term effects on these processes in Thau Lagoon. In contrast, the low resilience of the phytoplankton growth rate, related to the strong increase of growth a few days after the runoff, reaching higher levels than in the control, may lead to medium- to long-term impacts on the functioning and health of the lagoon's ecosystem, with consequences on provided services (e.g., oyster farming (**Dupuv** et al., 2000)).

During the heatwave experiment, the resilience dynamics were opposite to those observed during the terrestrial runoff experiment. Indeed, the processes that displayed a good resilience during the terrestrial

runoff experiment (i.e., primary production, respiration, and phytoplankton loss rate) all showed a worse resilience after the heatwave, whereas the phytoplankton growth rate, which was not resilient due to overcompensation after the runoff, had a better resilience after the heatwave, immediately returning to the control level once the heatwave ended. Similar to resistance, this important difference in the resilience and recovery patterns observed between the heatwave and runoff experiments may be due to the two disturbances being different in nature and intensity. In the present study, these fundamental differences resulted in the two disturbances not having the same effect on the community composition. Indeed, while the runoff affected all phytoplankton functional groups similarly (Soulié et al., 2024), the heatwave changed the phytoplankton community composition by favoring better-adapted taxa at the expense of other groups (Soulié et al., 2022a). Diatoms, prymnesiophytes, and cyanobacteria were favored by the heatwave. Meanwhile, dinoflagellates were negatively affected. Such important changes within the structure of the phytoplankton community must have played a major role in the lower resilience reported after the heatwave compared to that after the terrestrial runoff, owing to the well-established link between functional and compositional recoveries across a broad range of ecosystems (Hillebrand & Kunze, 2020; Polazzo & Rico, 2021). In supporting of this, the PCA revealed different relationships between processes and phytoplankton pigments, suggesting various contributions of different phytoplankton functional groups to the overall functional resilience of the system. In addition to changes in phytoplankton community composition, zooplankton community composition was also altered differently by the disturbances, as the heatwave favored harpacticoids at the expense of calanoid copepods (Zervoudaki et al., 2024), whereas the terrestrial runoff favored molluscs, rotifers, and copepod larvae (Courboulès et al., 2023). These varying effects likely contributed to the observed differences in functional resilience and recovery patterns by cascading down to the lower trophic levels.

503

504

505

506

507

508

509

510

511

512

513

514

515

516

517

518

519

520

521

522

523

524

525

526

527

528

529

530

531

Overall, the findings from our experiments suggest that the functional resilience and recovery of coastal plankton communities from Thau Lagoon after heatwaves would be threatened by important modifications of the phytoplankton and zooplankton community structures, while the lesser effect of terrestrial runoffs on the phytoplankton community structure would ensure better functional resilience after such events.

An important finding of the present study was that the effects of the terrestrial runoff and marine heatwave on community respiration were not significantly different. This means that two disturbances, very different in nature, intensity, and in how they affected environmental conditions, led to a similar response of

community respiration, as also seen with very similar Cohen's d effect sizes. This result was unexpected as plankton community respiration has been shown to strongly depend on both temperature (Sampou et al., 1994; Regaudie-de-Gioux & Duarte, 2012; Vaquer-Sunyer & Duarte, 2013) and light (Pringault et al., 2009; Mercado et al., 2014), both of which were affected very differently by the runoff and the heatwave. Additionally, the response of R was not related to similar environmental and pigment drivers during the resilience period of the two experiments, suggesting different driving factors. The response of chlorophylla differed significantly between the terrestrial runoff and heatwave experiments, indicating that the similar patterns observed in community respiration were not driven by changes in phytoplankton biomass. Similarly, community respiration normalized by bacterial biomass responded differently between the two experiments, suggesting that bacterial dynamics were also not responsible for the similar community respiration response. Community respiration is performed by both heterotrophic and autotrophic organisms in temperate coastal waters (Mantikci et al., 2024), and the contributions of bacteria (11-52%), protozooplankton (15-36%), phytoplankton (7.8-40%) and metazooplankton (3-9.4%) to total community respiration was shown to vary considerably depending on the studied system (Robinson & Williams, 2005). While it is not possible to assess which planktonic community contributed the most to the overall response of the community respiration toward the terrestrial runoff and the heatwave, the present study suggests that a common pattern of response exists for community respiration when exposed to a disturbance related to extreme weather events in Thau Lagoon, even if both phytoplankton and bacterial biomass responded differently depending on the disturbance. It is interesting to note that this pattern of response of respiration was also observed for a +4°C simulated heatwave with a coastal plankton community from the Gulf of Finland (Soulié et al., in prep). In this regard, further studies should be conducted to asses wether this pattern is also reported for other disturbances and other environmental conditions (different seasons, communities, etc.), and, if it is the case, it would suggest that it is primary production, more than respiration, that would dictate the fate of the global biogeochemical oxygen and carbon cycles in response to extreme weather events in coastal waters.

Broader implications, limitations, and future directions

532

533

534

535

536

537

538

539

540

541

542

543

544

545

546

547

548

549

550

551

552

553

554

555

556557

558559

560

561

The findings of the present study have important implications for understanding how Mediterranean coastal ecosystems might respond to the increasing frequency of extreme climatic events. While marine heatwaves are often perceived as the most severe threat to coastal ecosystems (e.g., Babcock et al. (2019)),

our results suggest that terrestrial runoff events could have more immediate and severe impacts on phytoplankton and processes mediated by plankton communities. Managing terrestrial runoff, particularly in the context of land-use changes and agricultural practices, may be crucial for maintaining ecosystem stability in coastal areas. Our study highlights the need for more proactive management strategies aimed at reducing terrestrial loads into coastal waters. Effective land-use management, improved wastewater treatment, and restoration of natural vegetation buffers along coastlines could mitigate the impacts of terrestrial runoff on coastal ecosystems, as emphasized in previous studies (e.g., Crain et al., 2009; Frigstad et al., 2023; Joseph 2024).

562

563

564

565

566

567

568

569

570

571

572

573

574

575

576

577

578

579

580

581

582

583

584

585

586

587

588

589

590

The observed resilience and overcompensation following runoff events suggest that although these disturbances are disruptive, the system has the potential to recover. This underscores the importance of implementing strategies to prevent chronic terrestrial loading, which could push ecosystems beyond their recovery capacities. In contrast, marine heatwaves, although less immediately disruptive in the short term, may have more persistent and long-lasting impacts on plankton dynamics, based on the low resilience found during the present study. Given the projected increase in the frequency and intensity of marine heatwaves due to global warming, this presents a challenge for long-term management. Our findings suggest that management efforts should prioritize enhancing ecosystem resilience to thermal stress, notably by conserving biodiverse areas—such as marine protected areas encompassing diverse habitats—which can serve as refugia for thermally tolerant species. Promoting connectivity between these areas and surrounding ecosystems may facilitate the recolonization of impacted zones by tolerant species following heatwave events. Reducing other stressors, such as overfishing and pollution, could help bolster the resilience of plankton communities to future heatwayes. An integrated approach to managing Mediterranean coastal waters should account for both marine heatwaves and terrestrial runoffs. Terrestrial runoffs and marine heatwayes do not typically occur simultaneously in the Mediterranean region (Durrieu de Madron et al., 2011). Therefore, they are expected to have cumulative rather than interactive effects, and therefore would generally impact different planktonic communities. Future studies should consider seasonal variability in the composition of plankton communities while investigating the short-term legacies of extreme weather events on plankton communities in coastal ecosystems. Additionally, this study was conducted over a relatively short timescale, and long-term experiments could help elucidate the chronic effects of repeated disturbances and their cumulative effects on plankton communities. For instance, previous research has highlighted the

importance of long-term monitoring to capture the full spectrum of plankton communities' responses to climate extremes, such as marine heatwaves (Evans et al., 2020; Gubanova et al., 2022; Deschamps et al., 2024), droughts (Marques et al., 2014), and storms (Hoover et al., 2006; Reyna et al., 2017; Calderó-Pascual et al., 2020).

The findings of the present study highlight the complex interplay between resistance and resilience in shaping the response of plankton oxygen metabolic parameters, phytoplankton growth, and loss rates to extreme weather disturbances in coastal waters. This knowledge may be useful for informing sustainable management practices to promote ecosystem stability in the context of the increased frequency and intensity of extreme climatic events in marine ecosystems.

Acknowledgements

We would like to thank all the participants to the mesocosm experiments, and especially Sébastien Mas and Justine Courboulès, for helping in running the experiments and participating to daily sampling, David Parin, for helping set up the high-frequency sensors and retrieve their data, and Florian Voron, for helping with the manual sampling of the mesocosms and for performing the nutrient analyses.

CRediT Author Contributions

Conceptualization: TS, FV, BM; Data curation: TS; Formal analysis: TS; Funding acquisition: FV, BM; Investigation: TS, FV, BM; Methodology: TS, FV, BM; Project administration: FV, BM; Ressources: FV, BM; Software: TS; Supervision: FV, BM; Validation: FV, BM; Visualization: TS; Writing – Original draft preparation: TS; Writing – Review & editing: TS, FV, BM

Funding Funding

The HW experiment was funded under the AQUACOSM project, which have received funding from the European Union's Horizon 2020 Research and Innovation Program (H2020/2017-2020) under grant agreement n°731065. The T. Runoff experiment was funded by the RESTORE project which have received funding from the French National Research Agency under grant agreement n°ANR-19-CE32-0013.

618	Conflict of interest disclosure
619 620 621	The authors declare that they have no conflicts of interest in relation to the content of the article.
622	Data availability statement
623	The dataset from the T. Runoff experiment and the dataset from the HW experiment are published in the
624	public database SEANOE (Soulié et al., 2023b; 2025): https://www.seanoe.org/data/00861/97260/ and
625	https://www.seanoe.org/data/00965/107675/
626	
627	References
628	
629	Ahme, A., A. Happe, M. Striebel, M. J. Cabrerizo, M. Olsson, J. Giesler, R. Schulte-Hillen, A. Sentimenti, N.
630	Kühne, and U. John. 2024. Warming increases the compositional and functional variability of a
631	temperate protist community. Sci. Tot. Env. 926: 171971. Doi:10.1016/j.scitotenv.2024.171971
632	Aminot, A., and R. Kérouel. 2007. Dosage automatique des nutriments dans les eaux marines, Méthodes en flux
633	continu, edited by: Ifremer, 336 pp, ISBN 2-84433-133-5
634	Babcock, R. C., R. H. Bustamante, E. A. Fulton, D. J. Fulton, M. D. E. Haywood, A. J. Hobday, R. Kenyon, R. J.
635	Matear, E. E. Plaganyi, A. J. Richardson, and M. A. Vanderklift. 2019. Severe continental-scale impacts
636	of climate change are happening now: Extreme climate events impact marine habitat forming
637	communities along 45% of Australia's coast. Front. Mar. Sci. 6:411. Doi:10.3389/fmars.2019.00411
638	Bas-Silvestre, M., M. Anton-Pardo, D. Boix, S. Gascon, J. Compte, J. Bou, B. Obrador, and X. D. Quintana. 2024.
639	Phytoplankton composition in Mediterranean confined coastal lagoons: testing the use of ecosystem
640	metabolism for the quantification of community-related variables. Aquat. Sci. 86:71.
641	Doi:10.1007/s00027-024-01084-9
642	Basu, S., and K. R. M. Mackey. 2018. Phytoplankton as key mediators of the biological carbon pump: Their
643	responses to a changing climate. Sustainability 10(3):869. Doi:10.3390/su10030869
644	Beaugrand, G., C. Luczak, and M. Edwards. 2009. Rapid biogeographical plankton shifts in the North Atlantic
645 646	Ocean. <i>Glob. Change Biol.</i> 15 (7):1790-1803. Doi:10.1111/j.1365-2486.2009.01848.x Bittig, H., C., A. Körtzinger, C. Neill, E. Van Ooijen, J. N. Plant, J. Hahn, and others. 2018. Oxygen optode
647	sensors: Principles, characterization, calibration, and application in the ocean. <i>Front. Mar. Sci.</i> 4 :429.
648	Doi:10.3389/fmars.2017.00429
649	Brussaard, C. P. D. 2004. Viral control of phytoplankton populations – a review. <i>J. Euk. Microb.</i> 51 (2): 125-138.
650	Doi:10.1111/j.15550-7408.2004.tb00537.x
651	Cabrerizo, M. J., J. M. Medina-Sanchez, J. M. Gonzalez-Olalla, D. Sanchez-Gomez, and P. Carillo. 2022.
652	Microbial plankton responses to multiple environmental drivers in marine ecosystems with different
653	phosphorus limitation degrees. Sci. Tot. Environ. 816:151491. Doi:10.1016/j.scitotenv.2021.151491
	· · · · · · · · · · · · · · · · · · ·

- 654 Calbet, A., and M. R. Landry. 2004. Phytoplankton growth, microzooplankton grazing, and carbon cycling in marine systems. *Limnol. Oceanogr.* **49**(1): 51-57. Doi:10.4319/lo.2004.49.1.0051
- 656 Calderó-Pascual, M., E. de Eyto, E. Jennings, M. Dillane, M. R. Andersen, S. Kelly, H. L. Wilson, and V.
- McCarthy. 2020. Effects of consecutive extreme weather events on a temperate dystrophic lake: A
- detailed insight into physical, chemical and biological responses. Water 12:1411.
- 659 Doi:10.3390/w12051411
- 660 Cohen, J. 1977. Statistical power analysis for the behavioral sciences revised. Edn Academic Press.
- 661 Courboulès, J., F. Vidussi, T. Soulié, E. Nikiforakis, M. Heydon, S. Mas, F. Joux, and B. Mostajir. 2023. Effects
- of an experimental terrestrial runoff on the components of the plankton food web in a Mediterranean
- 663 coastal lagoon. Front. Mar. Sci. 10:1200757. Doi:10.3389/fmars.2023.1200757
- 664 Crain, C. M., B. S. Halpern, M. W. Beck, and C. V. Kappel. 2009. Understanding and managing human threats
- to the coastal marine environment. Annals of the New York Academy of Sciences 1162:39-62.
- 666 Doi:10.1111/j.1749-6632.2009.04496.x
- Darmaraki, S., D. Denaxa, I. Theodorou, E. Livanou, D. Rigatou, E. Raitsos, and others. 2024. Marine heatwaves
- in the Mediterranean sea: A literature review. *Med. Mar. Sci.* 25(3):586-620. Doi:10.12681/mms.38392
- Deschamps, M. M., M. Boersma, and L. Giménez. 2024. Responses of the mesozooplankton community to marine
- heatwaves: Challenges and solutions based on a long-term time series. J. Animal Ecol.
- 671 Doi:10.1111/1365-2656.14165
- Duarte, P., J. M. Bernardo, A. M. Costa, F. Macedo, G. Calado, and L. Cancela da Fonseca. 2002. Analysis of
- 673 coastal lagoon metabolism as a basis for management. Aquat. Ecol. 36: 3-19.
- 674 Doi:10.1023/A:1013394521627
- Dupuy, C., A. Vaquer, T. Lam-Höai, C. Rougier, N. Mazouni, J. Lautier, Y. Collos, and S. Le Gall. 2000. Feeding
- 676 rate of the oyster Crassostrea gigas in a natural planktonic community of the Mediterranean Thau
- 677 Lagoon. Mar. Ecol. Prog. Ser. 205:171-184. Doi:10.3354/meps205171
- Durrieu de Madron, X., C. Guieu, R. Sempéré, P. Conan, D. Cossa, F. D'Ortenzio, and others. 2011. Marine
- ecosystems' responses to climatic and anthropogenic forcings in the Mediterranean. *Prog. Oceanogr.*
- **91**(2):97-166. Doi:10.1016/j.pocean.2011.02.003
- 681 Evans, R., M.-A. Lea, M. A. Hindell, and K. M. Swadling. 2020. Significant shifts in coastal zooplankton
- populations through the 2015/16 Tasman Sea marine heatwave. Est. Coast. Shelf Sci. 235:106538.
- 683 Doi:10.1016/j.ecss.2019.106538
- Falkowski, P. G., E. A. Laws, R. T. Barber, and J. W. Murray. 2003. Phytoplankton and their role in primary,
- new, and export production. In: Fasham, M. J. R. (Eds) Ocean biogeochemistry. Global change The
- 686 *IGBP Series*. Springer, Berlin, Heidelberg. Doi:10.1007/978-3-642-55844-3_5
- 687 Ferrarin, C., M. Bajo, D. Bellafiore, A. Cucco, F. De Pascalis, M. Ghezzo, and G. Umgiesser. 2014. Toward
- 688 homogenization of Mediterranean lagoons and their loss of hydrodiversity. Geophys. Res. Lett.
- **41**(16):5935-5941. Doi:10.1002/2014GL060843
- 690 Filiz, N., U. Iskın, M. Beklioglu, B. Öglü, Y. Cao, T. A. Davidson, M. Søndergaard, T. L. Lauridsen, and E.
- Jeppesen. 2020. Phytoplankton community response to nutrients, temperatures, and a heat wave in
- 692 shallow lakes: An experimental approach. *Water* **12**:3394. Doi:10.3390/w12123394

- Frigstad, H., G. S. Andersen, H. C. Trannum, M. McGovern, L.-J. Naustvoll, Ø. Kaste, A. Deininger, and D. Ø.
- Hjermann. 2023. Three decades of change in the Skagerrak coastal ecosystem, shaped by eutrophication
- 695 and coastal darkening. Est. Coast. Shelf Sci. 283:108193. Doi:10.1016/j.ecss.2022.108193
- 696 Garrabou, J., D. Gomez-Gras, A. Medrano, C. Cerrano, M. Ponti, R. Schlegel, and others. 2022. Marine heatwaves
- drive recurrent mass mortalities in the Mediterranean Sea. Glob. Change Biol. 28: 5708-5725.
- 698 Doi:10.1111/gcb.16301
- Gubanova, A., K. Goubanova, O. Krivenko, K. Stefanova, O. Garbazey, V. Belokopytov, T. Liashko, and E.
- Stefanova. 2022. Response of the Black Sea zooplankton to the marine heatwave 2010: Case of the
- 701 Sevastopol Bay. J. Mar. Sci. Eng. **10**(12):1933. Doi:10.3390/jmse10121933
- Hays, G., C., A.J. Richardson, and C. Robinson. 2005. Climate change and marine plankton. *Trends Ecol. Evol.*
- 703 **20**(6):337-344. Doi:10.0116/j.tree.2005.03.004
- Hillebrand, H., S. Langenheder, K. Lebret, E. Lindström, Ö. Östman, and M. Striebel. 2018. Decomposing
- multiple dimensions of stability in global change experiments. Ecol. Lett. 21:21-30.
- 706 Doi:10.1111/ele.12867
- Hillebrand, H., and C. Kunze. 2020. Meta-analysis on pulse disturbances reveals differences in functional and
- 708 compositional recovery across ecosystems. *Ecol. Lett.* **23**(3):575-585. Doi: 10.1111/ele.13457
- Holmes, R. M., A. Aminot, R. Kérouel, B. A. Hooker, and B. J. Peterson. 1999. A simple and precise method for
- 710 measuring ammonium in marine and freshwater ecosystems. Can J. Fish. Aquat. Sci. **56**: 1801-1808.
- 711 Doi:10.1139/f99-128
- Hoover, R. S., D. Hoover, M. Miller, M. R. Landry, E. H. DeCarlo, and F. T. Mackenzie. 2006. Zooplankton
- 713 response to storm runoff in a tropical estuary: bottom-up and top-down controls. *Mar. Ecol. Prog. Ser.*
- 714 **318**:187-201. Doi:10.3354/meps318187
- Huỳnh, T.-H., Z. Horváth, K. Pálffy, V. Kardos, B. Szabo, P. Dobosy, and C. F. Vad. 2024. Heatwave-induced
- functional shifts in zooplankton communities result in weaker top-down control on phytoplankton. *Ecol.*
- 717 Evol. **14**(8): e70096. Doi:10.1002/ece3.70096
- Jankowski, K. J., F. H. Mejia, J. R. Blaszczak, and G. R; Holtgrieve. 2021. Aquatic ecosystem metabolism as a
- 719 tool in environmental management. WIREs Water 8:e1521. Doi:10.1002/wat2.1521
- Jeppesen, E., J. Audet, T. A. Davidson, E. M. Neif, Y. Cao, N. Filiz, and others. 2020. Nutrient loading,
- temperature and heat wave effects on nutrients, oxygen and metabolism in shallow lake mesocosms pre-
- 722 adapted for 11 years. *Water* **13**:127. Doi:10.3390/w13020127
- 723 Joseph, S. Coastal darkening and eutrophication along the Swedish coast. Master thesis. Halmstad University,
- Sweden. https://urn.kb.se/resolve?urn=urn:nbn:se:hh:diva-54301
- La Jeunesse, I., C. Cirelli, H. Sellami, D. Aubin, R. Deidda, and N. Baghdadi. 2015. Is the governance of the Thau
- 726 coastal lagoon ready to face climate change impacts? Ocean Coast. Manag. 118(B): 234-246.
- 727 Doi:10.1016/j.ocecoaman.2015.05.014
- Landry, M. R., K. E. Selph, A. G. Taylor, M. Décima, W. M. Balch, and R. R. Bidigare. 2011. Phytoplankton
- growth, grazing and production balances in the HNLC equatorial Pacific. Deep Sea Res. II: Top. Stud.
- 730 Oceanogr. **58**(3-4): 524-535. Doi:10.1016/j.dsr2.2010.08.011

- 731 Lejeusne, C., P. Chevaldonné, C. Pergent-Martini, C. F. Boudouresque, and T. Pérez. 2010. Climate change
- effects on a miniature ocean: the highly diverse, highly impacted Mediterranean Sea. *Trends Ecol. Evol.*
- 733 **25**(4): 250-260. Doi:10.1016/j.tree.2009.10.009
- Liess, A., O. Rowe, S. N. Francoeur, J. Guo, K. Lange, A. Schröder, B. Reichstein, R. Lefèbure, A. Deininger, P.
- Mathisen, and C. L. Faithfull. 2016. Terrestrial runoff boosts phytoplankton in a Mediterranean coastal
- lagoon, but these effects do not propagate to higher trophic levels. *Hydrobiologia* **766**: 275-291.
- 737 Doi:10.10007/s10750-015-2461-4
- López-Urrutia, A., E. E. San Martin, R. P. Harris, and X. Irigoien. 2006. Scaling the metabolic balance of the
- 739 oceans. *Proc. Natl. Acad. Sci. USA* **103:**8739-8744. Doi:10.1073/pnas.0601137103
- 740 Mantikci, M., M. Bentzon-Tillia, J. Traving, H. Knudsen-Leerbeck, L. Riemann, J. L. S. Hansen, and S.
- Markarger. 2024. Plankton community metabolism variations in two temperate coastal waters of
- 742 contrasting nutrient richness. J. Geophys. Res.: Biogeosci. 129:e2023JG007919.
- 743 Doi:10.1029/2023JG007919
- Marques, S. C., A. L. Primo, F. Martinho, U. M. Azeiteiro, and M. A. Pardal. 2014. Shifts in estuarine zooplankton
- variability following extreme climate events: A comparison between drought and regular years. *Mar*.
- 746 *Ecol. Prog. Ser.* **499**:65-76. Doi:10.3354/meps10635
- Mercado, J. M., C. Sobrino, P. J. Neale, M. Segovia, A. Reul, A. L. Amorim, and others. 2014. Effect of CO₂,
- nutrients and light on coastal plankton. II. Metabolic rates. *Aquat. Biol.* 22:43-57. Doi:10.3354/ab00606
- Meunier, C., A. Liess, A. Andersson, S. Brugel, J. Paczkowska, H. Rahman, B. Skoglund, and O.F. Rowe. 2017.
- Allochtonous carbon is a major driver of the microbial food web- A mesocosm study simulating elevated
- 751 terrestrial matter runoff. Mar. Environ. Res. 129:236-244. Doi:10.1016/j.marenvres.2017.06.008
- Meyneng, M., H. Lemmonnier, R. Le Gendre, G. Plougoulen, F. Antypas, D. Ansquer, and others. 2024.
- Subtropical coastal microbiome variations due to massive river runoff after a cyclonic event. *Environ*.
- 754 *Microb.* **19**:10. Doi:10.1186/s40793-024-00554-9
- Mitchell, C., D. Drapeau, S. Pinkham, and W. M. Balch. 2024. A chlorophyll *a*, non-photochemical fluorescence
- quenching correction method for autonomous underwater vehicles in shelf sea environments. *Limnol*.
- 757 *Oceanogr. Methods* **22**(3):149-158. Doi:10.1002/lom3.10597
- 758 Mustaffa, N. I. H., L. Kallajoki, J. Biederbick, F. I. Binder, A. Schlenker, and M. Striebel. 2020. Coastal ocean
- darkening effects via terrigenous DOM addition on plankton: An indoor mesocosm experiment. *Front.*
- 760 *Mar. Sci.* **7**:547829. Doi:10.3389/fmars.2020.547829
- Navarro, D. 2015. Learning statistics with R: A tutorial for psychology students and other beginners. (Version
- 762 0.6). University of New South Wales, Sydney, Australia. R package version 0.5.1
- Paczkowska, J., S. Brugel, O. Rowe, R. Lefébure, A. Brutemark, and A. Andersson. 2020. Response of coastal
- phytoplankton to high inflows of terrestrial matter. Front. Mar. Sci. 7:80. Doi:10.3389/fmars.2020.00080
- Pecqueur, D., F. Vidussi, E. Fouilland, E. Le Floc'h, S. Mas, C. Roques, C. Salles, M.-G. Tournoud, and B.
- Mostajir. 2011. Dynamics of microbial planktonic food web components during a river flash flood in a
- 767 Mediterranean coastal lagoon. *Hydrobiologia* **673**:13-27. Doi:10.1007/s10750-011-0745-x
- Pérez-Ruzafa, A., A I. Fernandez, C. Marcos, J. Gilabert, J. I. Quispe, and J. A. Garcia-Charton. 2005. Spatial
- and temporal variations of hydrological conditions, nutrients and chlorophyll a in a Mediterranean
- 770 coastal lagoon (Mar Menor, Spain). *Hydrobiologia* **550**:11-27. Doi:10.1007/s10750-005-4356-2

- Pinheiro, J., D. Bates, and R Core Team. 2025. "Nlme: Linear and Nonlinear Mixed Effects Models." R Package
 Version 3.1–168 https://CRAN.R-project.org/package=nlme.
- Pringault, O., S. Tesson, and E. Rochelle-Newall. 2009. Respiration in the light and bacterio-phytoplankton coupling in a coastal environment. *Microb. Ecol.* **57**:321-334. Doi:10.1007/s00248-009-9422-7
- Polazzo, F., and A. Rico. 2021. Effects of multiple stressors on the dimensionality of ecological stability. *Ecol. Lett.* 24:1594-1606. Doi:10.1111/ele.13770
- Regaudie-de-Gioux, A., and C. M. Duarte. 2012. Temperature dependence of planktonic metabolism in the ocean.
 Glob. Biogeochem. Cyc. 26(1): GB1015. Doi:10.1029/2010GB003907
- Reyna, N. E., A. K. Hardison, and Z. Liu. 2017. Influence of major storm events on the quantity and composition of particulate organic matter and the phytoplankton community in a subtropical estuary, Texas. *Front.*Mar. Sci. 4:43. Doi:10.3389/fmars.2017.00043
- Robinson, C., P. Serret, G. Tilstone, E. Teira, M. V. Zubkov, A. P. Rees, and E. M. S. Woodward. 2002. Plankton respiration in the Eastern Atlantic Ocean. *Deep Sea Res. I: Oceanogr. Res. Pap.* **49**(5):787-813. Doi:10.1016/S0967-06375(01)00083-8
- Robinson, C., and P. J. le B. Williams. 2005. Respiration and its measurement in surface marine waters. In:
 Respiration in aquatic ecosystems. Eds: P. A. del Giorgio, and P. L. B. Williams. Oxford University
 Press, pp.147-180. Doi:10.1093/acprof:oso/9780198527084.003.0009
- Rodríguez, P., P. Byström, E. Geibrink, P. Hedström, F. Rivera Vasconcelos, and J. Karlsson. 2016. Do warming
 and humic river runoff alter the metabolic balance of lake ecosystems? *Aquat. Sci.* 78:717-725.
 Doi:10.1007/s00027-015-0463-y
- Rowe, O. F., J. Paczkowska, A. Brutemark, S. Brugel, S. J. Traving, R. Lefébure, and others. 2025. Climate
 change-induced terrestrial matter runoff may decrease food web production in coastal systems. *Limnol. Oceanogr.* Doi:10.1002/lno.12762
- Roy, S., C. A. Llewellyn, E. S. Egeland, and G. Johnsen. 2011. *Phytoplankton Pigments: Characterization,*chemotaxonomy and applications in oceanography. Cambridge, MA: Cambridge University Press.
- Sampou, P., and W. M. Kemp. 1994. Factors regulating plankton community respiration in Chesapeake Bay. *Mar. Ecol. Prog. Ser.* 110(2/3):249-258.
- Seneviratne, S. I., X. Zhang, M. Adnan, W. Badi, C. Dereczynski, A. Di Luca, and others. 2021. Weather and climate extreme events in a changing climate. In *Climate Change 2021: The Physical Science Basis*.

 Contribution of Working Group I to the Sixth Assessment Report of the Intergovernmental Panel on Climate Change [Masson-Delmotte, V., P. Zhai, A. Pirani, S.L. Connors, C. Péan, S. Berger, N. Caud, Y. Chen, L. Goldfarb, M.I. Gomis, M. Huang, K. Leitzell, E. Lonnoy, J.B.R. Matthews, T.K. Maycock, T. Waterfield, O. Yelekçi, R. Yu, and B. Zhou (eds.)]. Cambridge University Press, Cambridge, United
- Serret, P., C. Robinson, M. Aranguren-Gassis, E. E. Garcia-Martin, N. Gist, V. Kitidis, J. Lozano, J. Stephens, C.
 Harris, and R. Thomas. 2015. Both respiration and photosynthesis determine the scaling of plankton
 metabolism in the oligotrophic ocean. *Nat. Commun.* **6**:6961. Doi:10.1038/ncomms7961

Kingdom and New York, NY, USA, pp. 1513–1766, Doi:10.1017/9781009157896.013.

804

Soulié, T., S. Mas, D. Parin, F. Vidussi, and B. Mostajir. 2021. A new method to estimate planktonic oxygen metabolism using high-frequency sensor measurements in mesocosm experiments and considering daytime and nighttime respirations. *Limnol. Oceanogr. Methods* **19**:303-316. Doi:10.1002/lom3.10424

- Soulié, T., F. Vidussi, S. Mas, and B. Mostajir. 2022a. Functional stability of a coastal Mediterranean plankton
- community during an experimental marine heatwave. Front. Mar. Sci. 9:831496.
- 813 Doi:10.3389/fmars.2022.831496
- Soulié, T., F. Vidussi, J. Courboulès, S. Mas, and B. Mostajir. 2022b. Metabolic responses of plankton to warming
- during different productive seasons in coastal Mediterranean waters revealed by in situ mesocosm
- 816 experiments. Sci. Rep. 12: 9001. Doi:10.1038/s41598-022-12744-x
- 817 Soulié, T., F. Vidussi, S. Mas, and B. Mostajir. 2023a. Functional and structural responses of plankton
- 818 communities toward consecutive experimental heatwaves in Mediterranean coastal waters. Sci. Rep.
- 819 **13**:8050. Doi:10.1038/s41598-023-35311-4
- 820 Soulié, T., F. Vidussi, J. Courboulès, M. Heydon, S. Mas, F. Voron, C. Cantoni, F. Joux, B. Mostajir. 2023b.
- Dataset from a mesocosm experiment testing the effects of a terrestrial runoff on a Mediterranean
- plankton community. SEANOE. Doi:10.17882/97260
- 823 Soulié, T., F. Vidussi, J. Courboulès, M. Heydon, S. Mas, F. Voron, C. Cantoni, F. Joux, and B. Mostajir. 2024.
- Simulated terrestrial runoff shifts the metabolic balance of a coastal Mediterranean plankton community
- 825 towards heterotrophy. *Biogeosciences* **21**:1887-1902. Doi:10.5194/bg-21-1887-2024
- Soulié T., F. Vidussi, S. Mas, B. Mostajir. 2025. Dataset from an in situ mesocosm experiment testing the effects
- of a marine heatwave on a Mediterranean coastal plankton community. SEANOE. Doi:10.17882/107675
- Staehr, P.A., D. Bade, M.C. V. de Bogert, G.R. Koch, C. Williamson, P. Hanson, and others. 2010. Lake
- metabolism and the diel oxygen technique: state of the science. *Limnol. Oceanogr. Methods* **8**:628-644.
- 830 Doi:10.4319/lom.2010.8.0628
- Stibor, H., and M. Stockenreiter. 2023. Let there be light to interact. Front. Photobiol. 1:1284620.
- 832 Doi:10.3389/fphbi.2023.1284620
- 833 Striebel, M., L. Kallajoki, C. Kunze, J. Wollschläger, A. Deininger, and H. Hillebrand. 2023. Marine primary
- producers in a darker future: a meta-analysis of light effects on pelagic and benthic autotrophs. *Oikos*
- 835 e09501. Doi:10.1111/oik.09501
- Trinh, D. A., T. N. M. Luu, Q. H. Trinh, H. S. Tran, T. M. Tran, T. P. Quynh Le, and others. 2016. Impact of
- 837 terrestrial runoff on organic matter, trophic state, and phytoplankton in a tropical, upland reservoir.
- 838 Aguat. Sci. **78**:367-379. Doi:10.1007/s00027-015-0439-y
- 839 Trombetta, T., F. Vidussi, S. Mas, D. Parin, M. Simier, and B. Mostajir. 2019. Water temperature drives
- phytoplankton blooms in coastal waters. *PloS ONE* **14**(4):e0214933. Doi:10.1371/journal.pone.0214933
- Vaquer-Sunyer, R., and C. M. Duarte. 2013. Experimental evaluation of the response of coastal Mediterranean
- planktonic and benthic metabolism to warming. Est. Coasts 36:697-707. Doi:10.1007/s12237-013-9595-
- 843 2
- Vidussi, F., J.-C. Marty, and J. Chiavérini. 2000. Phytoplankton pigment variations during the transition from
- spring bloom to oligotrophy in the northwestern Mediterranean Sea. Deep Sea Res. I: Oceanogr. Res.
- 846 Papers 47:423-445. Doi:10.1016/S0967-0637(99)00097-7
- Vizzo, J. I., M. J. Cabrerizo, V. E. Villafañe, and E. W. Helbling. 2021. Input of terrestrial material into coastal
- Patagonian waters and its effects on phytoplankton communities from the ChubutRiver Estuary
- (Argentina). In: Häder, D. P., Helbling, E. W., Villafañe, V.E. (eds). Anthropogenic pollution of aquatic
- 850 *ecosystems*. Springer. Doi:10.1007/978-3-030-75602-4_7

851	Williams, le B. P. 1998. The balance of plankton respiration and photosynthesis in the open oceans. Nature 394:
852	55-57. Doi:10.1038/27878
853	Yalçın, G., D. Yıldız, M. Calderó-Pascual, S. Yetim, Y. Sahin, ME. Parakatselaki, F. Avcı, N. Karakaya, E. D.
854	Ladoukakis, S. A. Berger, K. A. Ger, E. Jeppesen, and M. Beklioğlu. 2024. Quality matters: Response of
855	bacteria and ciliates to different allochtonous dissolved organic matter sources as a pulsed disturbance
856	in shallow lakes. Sci. Tot. Env. 916:170150. Doi:10.1016/j.scitotenv.2024.1704